JOURNAL OF PROPULSION AND POWER
Vol. 10, No. 6, Nov.–Dec. 1994

Nonlinear Dynamic Simulation of Single- and Multispool Core Engines, Part I: Computational Method

M. T. Schobeiri,* M. Attia,† and C. Lippke†
Texas A&M University, College Station, Texas 77843

A new computational method for accurate simulation of the nonlinear, dynamic behavior of single- and multispool core engines, turbofan engines, and power-generation gas turbine engines is presented in Part I of this article. In order to perform the simulation, a modularly structured computer code has been developed that includes individual mathematical modules representing various engine components. The generic structure of the code enables the simulation of arbitrary engine configurations ranging from single-spool thrust generation to multispool thrust/power generation engines under adverse dynamic operating conditions. For precise simulation of turbine and compressor components, row-by-row calculation procedures were implemented that account for the specific turbine and compressor cascade and blade geometry and characteristics.

Nomenclature

C_f = friction coefficient
C_p, C_v = specific heat capacities
C_W = specific heat capacity of the wall
D_h = hydraulic diameter
h, H = static, total enthalpy
I = second moment of inertia of shaft
K = kinetic energy per unit mass
L = stage mechanical energy, length
l = specific mechanical energy
$\dot{m}$ = mass flow
p, P = static, total pressure
$\dot{Q}$ = rate of heat flow
R = gas constant
S = cross-sectional area
T, T^* = static, total temperature
T = stress tensor, $e_i e_j \tau_{ij}$
t = time
V = volume
V = absolute velocity vector
α = heat transfer coefficient
ε = convergence tolerance
κ = ratio of specific heats
μ = mass flow ratio, absolute viscosity
ρ = density
ω = angular velocity

Subscripts

A = air
C = convection
CA = air side convection
CG = gas side convection
c = cold
F = fuel
Fi = film
G = combustion gas
h = hot
I = inlet
i = shaft number
M = mixing
m = mechanical
O = outlet
P = primary
RF = flame radiation
S = segment, secondary
W = wall

Received April 17, 1993; presented as Paper 93-2580 at the AIAA/SAE/ASME/ASEE 29th Joint Propulsion Conference and Exhibit, Monterey, CA, June 28–30, 1993; revision received Nov. 23, 1993; accepted for publication Feb. 11, 1994.

*Professor, CFD-Propulsion Simulation Laboratory, Department of Mechanical Engineering. Member AIAA.

†Research Assistant, CFD-Propulsion Simulation Laboratory, Department of Mechanical Engineering.

I. Introduction

THE continuous improvement of the efficiency and performance of aircraft and power-generation gas turbine systems during the past decade has led to engine designs that are subject to extreme load conditions. Despite the enormous progress in the development of materials, at the design point, engine components operate near their aerodynamic, thermal, and mechanical load limits. Under these circumstances, any adverse dynamic operation causes excessive aerodynamic, thermal, and subsequent mechanical stresses that may affect the engine safety, reliability, and thus, the operability of the engine if adequate precautionary actions are not taken. Considering these facts, an accurate prediction of the above stresses and their cause is critical at the early stages of design and development of the engine and its components. One method of estimating the above stress situation is to utilize a data base, which is built on comprehensive tests of the performance, safety, and reliability of existing engine components. This method is not viable for estimating the dynamic behavior of a new generation of engines that incorporate components developed under a completely new design strategy. An alternative method for providing comprehensive information about the dynamic behavior of the engine under development is the use of a computational method capable of accurately predicting engine behavior under various dynamic conditions. A method with the above capability has been developed and will be discussed in this article. In order to perform the computational task, a large, generic, modularly structured computer code has been developed that is capable of precisely simulating the dynamic behavior of single and multispool core engines and their derivatives, such as bypass fan engines, turboprop engines, and power-generation gas turbine engines. In this article the theoretical background of the computational method, the code structure, the modular concept, and the levels of simulation are briefly discussed. In order to demonstrate the generic capability of the code, as representative examples, three different transient cases with zero-spool, single-, and multispool thrust and power-generation engines were

simulated. These transient cases vary from operation with fuel schedule, to extreme load changes, to total generator and turbine shutdown. For code validation, the simulation results are compared with the available measurements, and will be discussed in part II of this article.

II. Engine Simulation Background

Dynamic behavior of aircraft engines was investigated earlier by several researchers using the component performance map representation for engine simulation. Koenig and Fishbach[1] and Seldner et al.[2] utilized overall component performance maps in their simulation program GENENG, which performs purely steady-state computations. In order to account for system dynamics, Seller and Daniele[3] extended the above code by introducing simplified dynamic equations. A similar technique was also applied by Fawke et al.[4] In a report about hybrid simulation of single- and twin-spool turbofan engines, Szuch[5] also described the representation of engine components by overall performance maps. To estimate gas turbine starting characteristics, Agrawal and Yunis[6] generated a set of steady component characteristics, where the turbine and compressor components are represented by overall steady performance maps. Engine representation by performance maps, as briefly addressed above, and comprehensively discussed by Schobeiri,[7] exhibits a useful tool for approximating engine behavior within the operation range dictated by the component maps. However, the detailed information that is crucial for engine development and design cannot be provided at this simulation level. Furthermore, the above representation is not viable for providing the control system designer with the necessary input parameters, such as those describing the aerothermodynamic and structural conditions of the compressor and turbine blade rows. Consequently, the response of the real system to the intervention of the controller cannot be verified. These and other parameters are required inputs to the controller for triggering precautionary actions such as active surge control, achieved by adjusting variable compressor stator blades.

In order to address the above issues, Schobeiri[7-11] developed the modularly structured computer code COTRAN for simulating the nonlinear, dynamic behavior of single-shaft power-generation gas turbine engines. To account for the heat exchange between the material and the working fluid during a transient event, diabatic processes are employed in COTRAN for the combustion chamber and recuperator components. The dynamic expansion process through the turbine component is accomplished by a row-by-row calculation using the stage characteristics. COTRAN reflects real engine configurations and components, and is routinely used at the early stages of design and development of new gas turbine engines. Dynamic simulations of different single-shaft engines performed with COTRAN were reported by Schobeiri and Haselbacher,[12] and Schobeiri.[10,11] Although COTRAN represents an advanced, nonlinear, dynamic code, its simulation capability is restricted to single-shaft power-generation gas turbine engines, and thus, cannot be used for simulating multispool aircraft engines.

III. Development of a Generic Simulation Concept

The aforementioned circumstances motivated development of a new computational method with the corresponding, generic, modularly structured computer code for simulating the nonlinear dynamic behavior of single- and multispool high-pressure core engines, turbofan engines, and power-generation gas turbine engines. The code is capable of simulating aircraft engines having up to five spools with variable geometry, with or without additional power-generation shafts. A precise prediction of the dynamic behavior of the engine and the identification of critical parameters by the code enables the engine designer to take appropriate steps using sophisticated control systems. The code may also be used to proof the design concept of the new generation of high-performance engines. The modular structure of the code enables the user to independently develop new components and integrate them into the simulation code.

Based on the components utilized in the existing and possible future aircraft and power-generation gas turbine systems, a generic simulation concept has been developed that accounts for different types of engines. As shown in Fig. 1, several components are common to both thrust- and power-generation gas turbine engines such as inlet diffuser, exit nozzle, compressors, combustion chamber, turbines, and multiple shafts. For supersonic aeroengines, the supersonic diffuser and nozzle, as well as an afterburner, are added to the component list. Aside from the components listed above, there are a number of other components such as control systems, speed sensors, and pipes that are encountered in any type of engine.

Starting from the base engines shown in Fig. 1, various derivatives can easily be created by introducing additional components such as fans, propellers, ducts, or power-generating shafts. Thus, the derivatives exhibit different component arrangements. This procedure can be extended to zero-, single-, or multispool engines without restrictions.

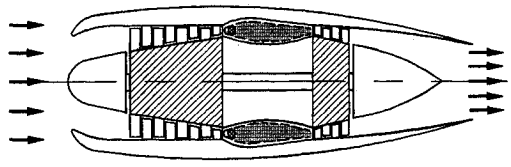

SINGLE-SPOOL BASE ENGINE

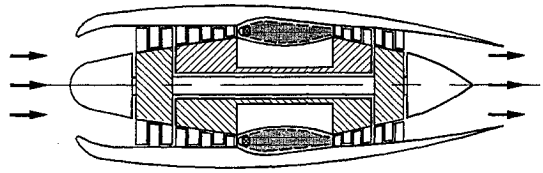

TWIN-SPOOL ENGINE

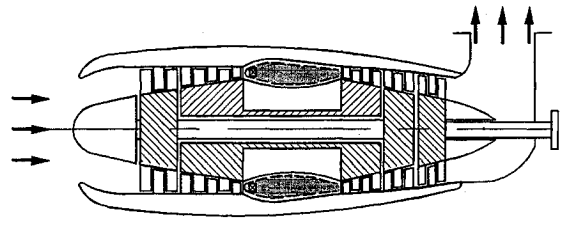

TWIN-SPOOL ENGINE WITH FREE TURBINE

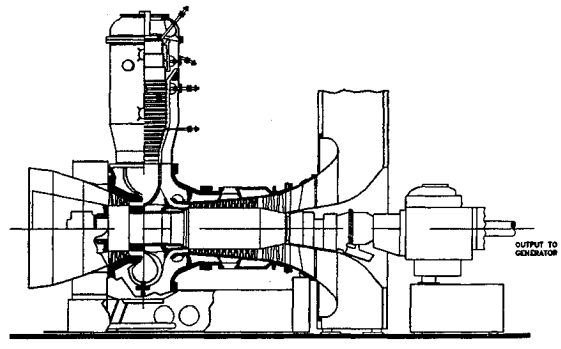

SINGLE-SPOOL POWER GENERATION ENGINE

Fig. 1 Survey of gas turbine engines.

A. Engine Components, Modular Concept, Module Identification

A schematic component arrangement and modeling of a two-spool core engine is shown in Fig. 2. The corresponding modules are implemented into the simulation code. Figure 3 displays a list of components with their corresponding module representations and symbols that are resident in the code. They exhibit the basic components essential for generically configuring any possible aero- and power-generation gas turbine engine. These modules are connected with a plenum, which is a coupling component between two or more successive components. The primary function of the plenum is to couple the dynamic information of entering and exiting components such as mass flow, total pressure, total temperature, fuel/air ratio, and water/air ratio. After entering the plenum a mixing process takes place, where the aforementioned quantities reach their equilibrium values. These values are the same for all outlet components exiting the plenum.

The above component survey has led to the practical conclusion that any aircraft or power-generation gas turbine engine and its derivatives, regardless of configuration (i.e., number of spools and components), can be simulated by arranging the components according to the engine configuration of interest. The present nonlinear dynamic code is based on this design concept and can generically simulate the transient behavior of existing and new engines and their derivatives. The modules are identified by their names, shaft number, and inlet and outlet plena. This information is vital for generating the system of differential equations representing individual modules. Modules are then combined into a complete system that corresponds to the engine configuration. Each module is physically described by the conservation laws of thermofluid mechanics that result in a system of nonlinear, partial differential, or algebraic equations. Since an engine consists of a number of components, its modular arrangement leads to a system containing a number of sets of equations. The above concept can be systematically applied to any aircraft or power-generation gas turbine engine.

The general application of the modular concept is illustrated in Fig. 4, where, systematically, more complex engine configurations are generated. The twin-spool engine shown in Fig. 4 exemplifies the modular extension of the single-spool base engine. It consists of two spools with the shafts S_1 and S_2, on which the low- and high-pressure components such as compressors and turbines are assembled. The two shafts are coupled by the working media air and combustion gas. They rotate with different speeds that are transferred to the control system by the sensors N_{s1} and N_{s2}. Air enters the inlet diffuser D_1, which is connected with the multistage compressor assembled on S_1, and is decomposed in several compressor stages C_{1i}. The first index 1, refers to the spool number and the second index i, marks the number of the compressor stage.

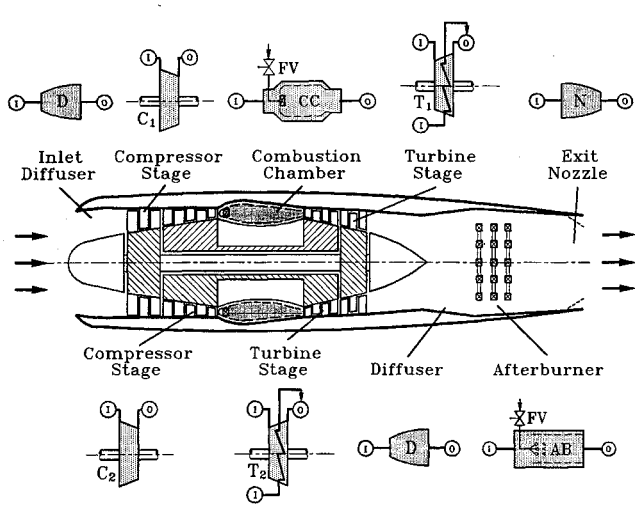

Fig. 2 Twin-spool engine module allocation.

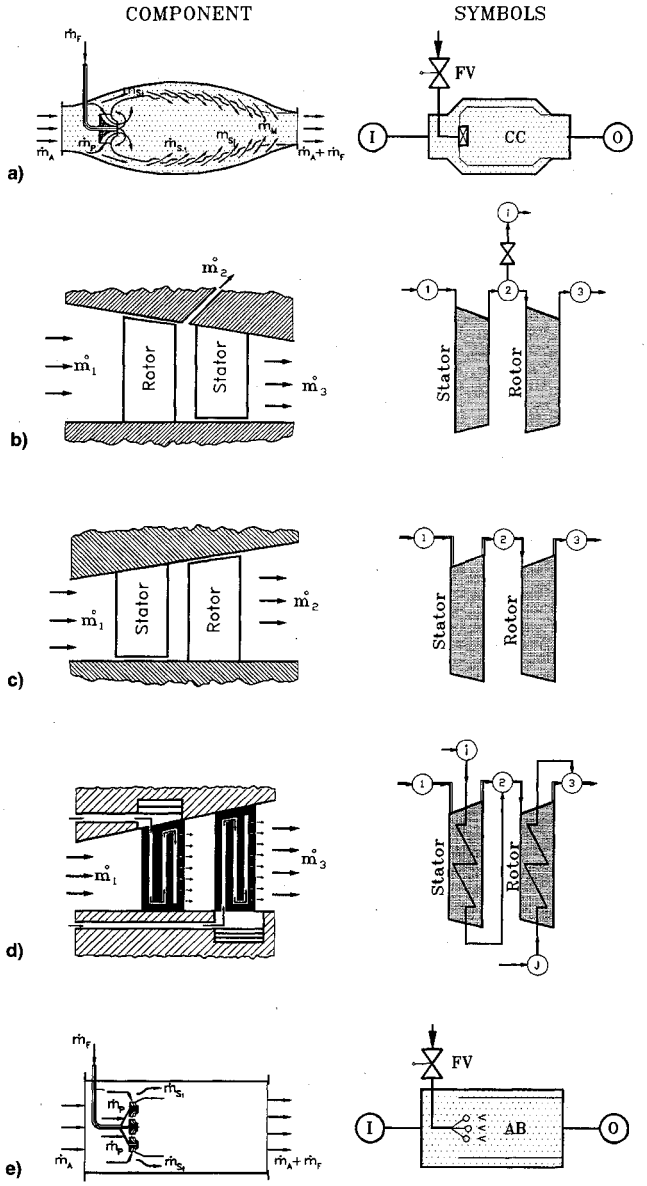

Fig. 3 Component representations: a) combustion chamber: *CC*, b) uncooled compressor stage: *C*, c) uncooled turbine stage: *T*, d) cooled turbine stage: *T*, and e) afterburner: *AB*.

After compression in the S_1 compressor stage group, the air enters the second compressor (HP-compressor) assembled on the S_2 shaft that consists of stages C_{21}–C_{25}. In the combustion chamber CC_1, high-temperature combustion gas is produced by adding fuel from the fuel tank FT. The gas expands in the high-pressure turbine that consists of stages T_{21}–T_{23}. By exiting from the last stage of HP-turbine, the combustion gas enters the low-pressure turbine consisting of stages T_{11}–T_{13} and is expanded through the exit nozzle. Two bypass valves BV_1 and BV_2 are connected with the compressor stator blades for surge prevention. The fuel valve FV_1 is placed between the fuel tank FT and the combustion chamber CC_1. The pipes P_i serve for cooling air transport from the compressor to cooled turbines. The compressor stage pressures, the turbine inlet temperature, and the rotor speed are the input signals to the control system, which controls the valve cross sections and the fuel mass flow.

B. Levels of One-Dimensional Simulation, Component Modeling

The degree of accuracy of a dynamic engine simulation is primarily determined by the level of component modeling and, consequently, the engine simulation complexity. Thus, the degree of accuracy increases with increasing the level of

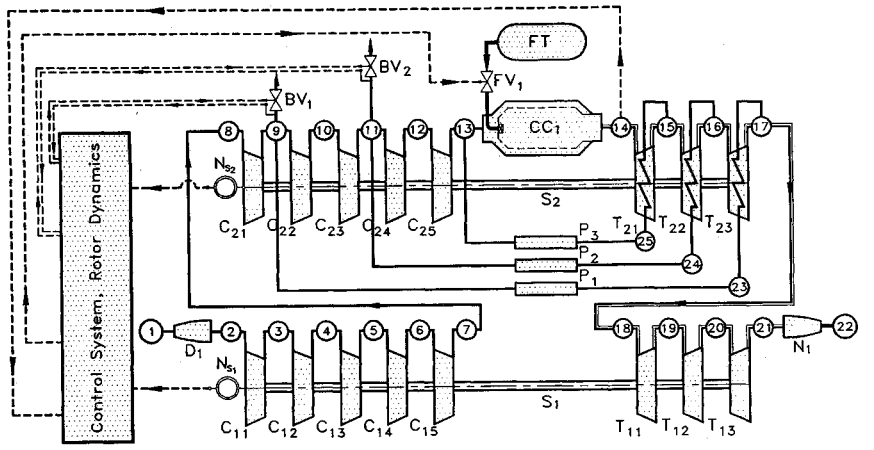

BV_i = Bypass valve
C_{ij} = j^{th} compressor stage, i^{th} spool
CC_i = Combustion Chamber
D_i = Diffuser
FT = Fuel Tank
FV_i = Fuel valve
N_i = Nozzle
Ns_i = Speed sensor
P_i = Pipes
S_i = Shaft
T_{ij} = j^{th} turbine stage, i^{th} spool
Signal flow
Air flow
Gas flow
Fuel flow

Fig. 4 Schematic of a twin-spool base engine.

simulation complexity. Four simulation levels are introduced. The first level uses the steady-state component performance maps without dynamic coupling. The system simulation is described by a set of algebraic equations only. Examples of this level were presented in the first paragraph of Sec. II. Use of the compressor and turbine performance maps, and consideration of the component dynamics by introducing the plenum as the coupling component, characterizes the second level of simulation, in which algebraic and ordinary differential equations describe the system. A third level of simulation is defined by utilizing the conservation laws of thermofluid dynamics in differential form to model the engine components. At this level, compressor and turbine components are adiabatically modeled in a row-by-row manner. The compression and expansion calculation processes through compressor and turbine rows are performed using the row geometry and flow characteristics, which include losses and efficiencies. Finally, the fourth level of simulation calculates the compressor and turbine blade temperatures. In this case diabatic processes are used that result in more than doubling the number of governing differential equations.

IV. Physical and Mathematical Description of the Components

The components within which thermo-fluid-dynamic processes take place are mathematically modeled by sets of partial differential equations or algebraic equations. These are

Equation of continuity

$$\frac{\partial \rho}{\partial t} = -\nabla\cdot(\rho V) \tag{1}$$

Equation of motion

$$\frac{\partial(\rho V)}{\partial t} + \nabla\cdot(\rho VV) = -\nabla p + \nabla\cdot T \tag{2}$$

Equation of total energy

$$\frac{\partial H}{\partial t} = -kV\cdot\nabla H - (\kappa - 1)\left[\frac{1}{\rho}\nabla\cdot(\rho V)(H + K) + \frac{V\cdot\partial(\rho V)}{\rho\partial t}\right] + \frac{\kappa}{\rho}\left[-\nabla\cdot\dot{q} + \nabla\cdot(V\cdot T)\right] \tag{3}$$

with T as the shear stress tensor, $H = h + V^2/2$, the total enthalpy, and $K = V^2/2$ the kinetic energy. The total enthalpy can be expressed in terms of total temperature:

$$c_p\frac{\partial T^*}{\partial t} = -kV\cdot\nabla(c_pT^*) - (\kappa - 1)\left[\frac{1}{\rho}\nabla\cdot(\rho V)(c_pT^* + K) + \frac{V\cdot\partial(\rho V)}{\rho\partial t}\right] + \frac{\kappa}{\rho}\left[-\nabla\cdot(\dot{q} + \nabla\cdot(V\cdot T)\right] \tag{4}$$

Finally, the total energy equation in terms of total pressure can be established by inserting Eqs. (1) and (2) into Eq. (3) with $P = p + \rho V^2/2$ as the total pressure:

$$\frac{\partial P}{\partial t} = -k\nabla\cdot(VP) - (\kappa - 1)[\nabla\cdot(\dot{q}) - \nabla\cdot(V\cdot T)] - (\kappa - 2)\frac{\partial(\rho K)}{\partial t} \tag{5}$$

For further treatment, these equations are written in the Cartesian coordinate system. The continuity equation is

$$\frac{\partial \rho}{\partial t} = \frac{\partial}{\partial x_i}(\rho V_i) \tag{6}$$

The equation of momentum is

$$\frac{\partial(\rho V_i)}{\partial t} = -\frac{\partial}{\partial x_j}(\rho V_iV_j) - \frac{\partial p}{\partial x_i} + \frac{\partial T_{ij}}{\partial x_j} \tag{7}$$

The energy equation in terms of total pressure

$$\frac{\partial P}{\partial t} = -\kappa \frac{\partial}{\partial x_i}(PV_i) - (\kappa - 1)\left[\frac{\partial \dot{q}_i}{\partial x_i} - \frac{\partial}{\partial x_i}(V_j T_{ij})\right] - (\kappa - 2)\frac{\partial(\rho K)}{\partial t} \tag{8}$$

Energy equation in terms of total temperature

$$c_p \frac{\partial T^*}{\partial t} = -kV_i \frac{\partial}{\partial x_i}(c_p T^*) - \frac{\kappa - 1}{\rho}\left[\frac{\partial}{\partial x_i}(\rho V_i)(c_p T^* + K) + V_i \frac{\partial(\rho V_i)}{\partial t}\right] + \frac{\kappa}{\rho}\left[-\frac{\partial \dot{q}_i}{\partial x_i} + \frac{\partial}{\partial x_i}(V_j T_{ji})\right] \tag{9}$$

in which the indices i and j represent the components in the Cartesian coordinate system.

The above equations are the general basis for the description of the nonlinear, dynamic behavior of the engine components. A three-dimensional solution for the entire engine simulation requires considerable computational efforts using massive parallel processing and will not likely be available in the near future. Two-dimensional treatment also requires a great computational effort. For integral engine simulation purposes, a one-dimensional approximation gives sufficiently accurate results. The partial differential Eqs. (6–9) can be approximated as ordinary differential equations by means of conversion into difference equations. These equations can then be solved numerically with the prescribed initial and boundary conditions. For this purpose, the flowfield is divided into a number of prescribed discrete zones. The above conservation laws will be applied to concrete cases discussed in Part II.

V. Modeling of Components

The above conservation laws of thermofluid dynamics describe the dynamic behavior of the engine components, resulting in a system of ordinary differential and algebraic equations. The components are modeled mathematically as modules for configuring a complete system of any thrust or power-generating gas turbine engine. According to their functions, the engine components are classified into four categories. Modules belonging to the first category of components exchange no thermal or mechanical energy with surroundings such as pipes and subsonic and supersonic diffusers and nozzles. The function of the diffuser and nozzle modules is the transfer of mass flow associated with the partial conversion of kinetic energy into potential energy and vice versa. The function of the pipe module is to transfer mass flow from one point to another. The cooling air supply for the rotor and turbine blade cooling purposes is a simple example for the application of the component pipe. Each module is identified by its name and its inlet and outlet plena, which function as component addresses. This module addressing convention is applied universally within the code.

The second category of modules includes components within which thermal energy conversion and exchange processes take place, such as combustion chambers, afterburners, recuperators, and coolers.

The third category of modules consists of those components within which conversion and exchange of thermal and mechanical energy take place, such as uncooled and cooled compressor and turbine stage modules. As an example, a cooled turbine stage with its inlet and outlet addresses are shown in Fig. 3d. The modules for cooled compressor and turbine stages represent the last stage of a high-pressure compressor and the first stage of a high-pressure turbine, respectively. For a multistage compressor or turbine the simulation is provided by a serial arrangement of these components. Unlike the cooled compressor stage where the cooling mass flow enters the cooler and does not participate in the compression process, the turbine cooling mass flow enters the plenum downstream of the turbine stage and is mixed with the turbine main stream combustion gas. The mixing process changes the fuel air/ratio that is calculated precisely.

The fourth category of modules consists of valves, sensors, control systems, fuel and load schedule generators, etc. Input information to the controller may contain rotor speed, turbine inlet temperature, pressure, and compressor inlet and exit pressures and temperatures. This information may trigger closing or opening of the fuel valves or bypass valves and perform other control functions, such as the adjustment of compressor stator blades required in active surge protection. For the transient simulation cases discussed in part II of this article, a simple control system is linked to the computational code. The controller has the rotor speed and the turbine inlet temperature as inputs. Controller output is the fuel mass flow. Finally, the shaft module represents the rotor speed behavior. The modules mentioned above are preliminary resident modules in the simulation code. New modules may be developed and added to the system. The representatives of each of these groups are briefly described below.

A. Modeling of Inlet, Exit, Pipes

The function of these components consists of, among other things, the transportation of mass flow, and, partially, the conversion of kinetic energy into potential energy and vice versa. For the application of the conservation laws to a duct with a variable cross section, the equation of continuity is written as

$$\frac{\partial \rho}{\partial t} = -\frac{1}{\Delta x}\left(\frac{\dot{m}_{i+1}}{S_{i+1}} - \frac{\dot{m}_i}{S_i}\right) \tag{10}$$

in which, in contrast to Eqs. (6–9), the indices i and $i + 1$, used in this section, represent the stations for one-dimensional calculation. The momentum equation then becomes

$$\frac{\partial \dot{m}_{i+1}}{\partial t} = -\frac{1}{\Delta x}(\dot{m}_{i+1}V_{i+1} - \dot{m}_i V_i + p_{i+1}S_{i+1} - p_i S_i) + \left[\left(\frac{\dot{m}_k V_k + p_k S_k}{S_k}\right)\left(\frac{S_{i+1} - S_i}{\Delta x}\right)\right] - c_f \frac{\dot{m}_{i+1}V_{i+1}}{2D_h} \tag{11}$$

where S_i is the cross-sectional area. In Eq. (2), the divergence of the shear stress tensor represents the shear forces acting on the surface. For a one-dimensional flow, the only nonzero term is $\partial\tau_{21}/\partial x_2$, which can be related to the wall shear stress τ_W. The wall shear stress in turn is a function of the friction coefficient c_f, which is directly related to the loss coefficient of the pertinent component under consideration. The energy equation is modified as follows:

$$\frac{\partial P_{i+1}}{\partial t} = -\frac{\kappa_K}{\Delta x}\left(\frac{\dot{m}_{i+1}P_{i+1}}{\rho_{i+1}S_{i+1}} - \frac{\dot{m}_i P_i}{\rho_i S_i}\right) - (\kappa_K - 1)c_{f_k}\frac{\dot{m}_{i+1}^3}{2\rho_{i+1}^2 S_{i+1}^3 D_{h_{i+1}}} - (\kappa_k - 2)\frac{\dot{m}_k}{\rho_k S_k^2} \times \left[\frac{1}{2}\frac{\dot{m}_k}{\rho_k}\frac{1}{\Delta x}\left(\frac{\dot{m}_{i+1}}{S_{i+1}} - \frac{\dot{m}_i}{S_i}\right) - \frac{\partial \dot{m}_{i+1}}{\partial t}\right] \tag{12}$$

with

$$\rho_k = \frac{1}{R}\frac{p_{i+1} + p_i}{T_{i+1} + T_i}; \quad C_{p_k} = \frac{H_{i+1} - H_i}{T_{i+1}^* - T_i^*}; \quad \kappa_k = \frac{C_{p_k}}{C_{p_k} - R}$$

where the quantities with the subscript k represent the averaged values between the stations i and $i + 1$. For a constant

cross section, the equations of continuity and motion are written respectively as

$$\frac{\partial \rho_{i+1}}{\partial t} = -\frac{1}{\Delta x S}(\dot{m}_{i+1} - \dot{m}_i) \tag{13}$$

$$\frac{\partial \dot{m}_{i+1}}{\partial t} = -\frac{1}{\Delta x}\left[\frac{\dot{m}_{i+1}^2}{\rho_{i+1}S} - \frac{\dot{m}_i^2}{\rho_i S} + S(p_{i+1} - p_i)\right] - c_f \frac{\dot{m}_{i+1}^2}{2\rho_{i+1} S D_h} \tag{14}$$

Similarly, the equation of energy is simplified to

$$\frac{\partial P_{i+1}}{\partial t} = -\frac{\kappa_K}{\Delta x S \rho_k}\left(\frac{\dot{m}_{i+1}P_{i+1}}{\rho_{i+1}} - \frac{\dot{m}_i P_i}{\rho_i}\right) - (\kappa_K - 1)c_f \frac{\dot{m}_{i+1}^3}{2\rho_{i+1}^2 S^3 D_h} - (\kappa_k - 2)\frac{\dot{m}_k}{\rho_k S^2} \times \left[\frac{1}{2}\frac{\dot{m}_k}{\rho_k}\frac{1}{\Delta x S}(\dot{m}_{i+1} - \dot{m}_i) - \frac{\partial \dot{m}_{i+1}}{\partial t}\right] \tag{15}$$

Eqs. (13–15) describe the transient process of a compressible flow within a tube with a constant cross section. For an incompressible flow, this system can be reduced to a single differential equation:

$$\frac{\partial \dot{m}}{\partial t} = \frac{R\dot{m}^2}{LS}\left(\frac{T_1}{p_1} - \frac{T_n}{p_n}\right) + \frac{S}{L}(p_1 - p_n) - c_f \frac{\dot{m}^2}{2\rho S D_h} \tag{16}$$

The friction coefficient c_f can be determined from the known steady-state condition.

B. Modeling of Combustion Chamber and Afterburner

A brief description of the combustion chamber as the representative example is given below. A combustor generally consists of a combustion zone, or primary zone, surrounded by n rows of segments, the cooling zone, and the mixing zone (Fig. 3a). The actual process of combustion occurs in the primary zone. The mixing in of cold air flowing through mixing nozzles, arranged radially, reduces the gas temperature in the mixing zone to a level acceptable for the gas turbine that follows. The rows of segments in the combustion zone are subjected to a severe thermal loading due to direct flame radiation. Film and/or convection cooling on both the air and the gas sides cools these segments. The air required to cool these hot segments flows through finned cooling channels, thereby contributing to the convection cooling of the segments on the air side. The cooling airflow exiting from the jth segment row effects the film cooling process on the gas side within the boundary layer in the next row of segments. At the end of that process, the cooling air mass flow should be mixed completely with the primary air mass flow. The mass flow relationships prevailing in the primary, the cooling, and the mixing zones are substituted into the energy equation, already formulated. Their effect is significant, particularly in the case of the energy balance, because they determine the temperature distribution in the individual combustion chamber stations. For that reason, we first determine the mass flow relationships and then deal with the energy balance.

1. *Mass Flow Balance*

The combustion chamber mass flow is divided into primary mass flow, secondary (cooling) mass flow, and mixing mass flow:

$$\dot{m}_p = \mu_p \dot{m}, \quad \dot{m}_S = \mu_S \dot{m}, \quad \dot{m}_M = \mu_M \dot{m} \tag{17}$$

If the primary zone consists of n rows of segments, the cooling mass flow for the jth row of segments is

$$\dot{m}_{S_j} = \mu_j \dot{m}_S = \mu_j \mu_S \dot{m} \tag{18}$$

If the fuel component $\mu_F = m_F/m$ is also taken into consideration, the mass flow within the jth row of segments is

$$\dot{m}_j = \sigma_j \dot{m}, \quad \sigma_j = \mu_F + \mu_p + \mu_S \sum_{\nu=1}^{j} \mu_\nu \tag{19}$$

To determine the transient behavior of a combustion chamber that has already been designed, it is necessary to start from the given ratios μ_p, μ_S, μ_M, and σ_j. For a new design, it is possible to vary these ratios until the desired solution is attained. The mass flow in the combustion chamber is obtained as the solution to the modified version of Eq. (11):

$$\frac{\partial \dot{m}}{\partial t} = \frac{R\dot{m}^2(1 + \mu_F)}{\Delta x S}\left[\left(\frac{T}{P}\right)_I - \left(\frac{T}{P}\right)_O\right] + \frac{S}{\Delta x}\left(\frac{P_I - P_O}{1 + \mu_F}\right) - c_f \frac{\dot{m}^2(1 + \mu_F)}{2\rho S D_h} \tag{20}$$

The volume of the combustion chamber is replaced here with an equivalent volume, with a constant cross section S and length Δx. The pressures and temperatures in Eq. (20) thus represent inlet and outlet parameters, which are specified by the indices I and O and must be known at the design point.

2. *Temperature Transients*

To determine the temperature transients for the fluid media within individual parts of the combustion chamber, we start from Eq. (9). Considering the air, fuel, and eventually, water as the main combustion components, the rearrangement of Eq. (9) reads:

$$\frac{\partial T_{i+1}^*}{\partial t} = \frac{1}{V\rho_{i+1}c_{p_{i+1}}}\left\{\sum_{k=1}^{K} \dot{m}_{ik}[\kappa_{i+1}(c_{p_i}T_i^*)_k - c_{p_{i+1}}T_{i+1}^*]\right\} + \frac{1}{V\rho_{i+1}c_{p_{i+1}}}[(1 - \kappa_{i+1})\dot{m}_{i+1}c_{p_{i+1}}T_{i+1}^* - \kappa_{i+1}\dot{Q}_G] - \left(\frac{1 - \kappa_{i+1}}{c_{p_{i+1}}}\right)\left(\frac{\dot{m}}{\rho^2 S^2}\right)_{i+1}\frac{\partial \dot{m}_{i+1}}{\partial t} \tag{21}$$

with $\dot{Q}_G = V\Delta\dot{Q}$.

The index i refers to the computation station in question. The mixing components are identified with the sequential index k, the upper summation limit for which K represents the number of components involved in a mixing process. The mixing components at the inlet station are the cooling air, the combustion air, and the fuel. For the cooling zone, Eq. (9) yields:

$$\frac{\partial T_{i+1}^*}{\partial t} = \frac{\kappa}{V\rho c_p}[\dot{m}c_p(T_i^* - T_{i+1}^*) - \dot{Q}_A] + \frac{1 - \kappa}{c_p}\left(\frac{\dot{m}}{\rho^2 S^2}\right)\frac{\partial \dot{m}}{\partial t} \tag{22}$$

with $\dot{Q}_A = V\Delta\dot{Q}$.

The temperature distribution within the segment material can be determined as follows using the heat conductance equation:

$$\frac{d\bar{T}_W}{dt} = \frac{1}{\rho_W c_W V_W}(\dot{Q}_h + \dot{Q}_c) \tag{23}$$

The heat flows $\dot{Q}_G$, $\dot{Q}_A$, $\dot{Q}_h$, and $\dot{Q}_c$ are those supplied to or carried off from the part of the system. For the primary zone surrounded by a row of segments, $\dot{Q}_G$ is made up of the fuel heat $\dot{Q}_F$, the flame radiation heat $\dot{Q}_{RF}$, and the convection heat $\dot{Q}_{CG}$, on the gas (or hot) side. The increased temperature level produced in the segments from the direct flame radiation is reduced to an acceptable level by an intensive film cooling on the gas side and convective heat removal on the air side. The segments are therefore subjected to the following thermal loading on the gas side (or hot side):

$$\dot{Q}_h = \dot{Q}_{RF} + \dot{Q}_{Fi} \tag{24}$$

with $\dot{Q}_{Fi}$ standing for the amount of heat carried off by the film cooling. The heat flow carried off on the air side $\dot{Q}_c$ consists of a convection and a radiation component. The latter is due to the difference in temperature between the cold air enclosure liner and the warm surface of the fins. As a result, the heat flow carried off on the air side is

$$\dot{Q}_c = \dot{Q}_{CA} + \dot{Q}_{RA} \tag{25}$$

For the film cooling

$$\dot{Q}_{F_i} = \bar{\alpha}_{F_i} S_G (\bar{T}_{F_i} - \bar{T}_W) \tag{26}$$

in which $\bar{\alpha}_{F_i}$ is the average heat transfer coefficient and $\bar{T}_{Fi}$ the average film temperature, from Schobeiri.[11,13] The convection heat removal on the air side is obtained from

$$\dot{Q}_{CA} = \bar{\alpha}_A S_A (\bar{T}_W - \bar{T}_A) \tag{27}$$

The radiation heat flows $\dot{Q}_{RA}$, $\dot{Q}_{RF}$ have been determined from Schobeiri[13]:

$$\dot{Q}_G = \dot{Q}_F \doteq \dot{Q}_{RF} + \dot{Q}_{CG} \tag{28}$$

C. Modeling of Turbine and Compressor Components

During dynamic operation, the uncooled turbine and compressor blades undergo a heat transfer process between the materials subjected to the flow, e.g., the blading and the fluid medium. A similar process occurs for cooled turbine and compressor blades during steady state and dynamic operation. In order to take this heat transfer into consideration, the components must be divided into their individual rows or stages. For the turbine component, the row-by-row expansion calculation method by Schobeiri[14] and Schobeiri and Abouelkheir[15] is used, where the row efficiency at off-design points is determined for the given turbine blade geometry and the flow angles calculated from row-velocity diagrams. For the compressor component, a row-by-row compression calculation method may be applied. For subsonic and transonic compressors, the off-design efficiencies are calculated from the total loss correlations as a function of the modified diffusion factor. The nonlinear dynamic behavior of these components is described by the conservation laws in conjunction with the known row characteristics. For the special case in which there are no discontinuities and no changes in the mass flow or mixing processes within the row, Eq. (9) is reduced to

$$\frac{\partial T^*_{i+1}}{\partial t} = -\frac{k}{\rho V c_{p_{i+1}}} (\dot{m}_{i+1} c_{p_{i+1}} T^*_{i+1} - \dot{m}_i c_{p_i} T^*_i + \dot{Q}_R + L_R) \tag{29}$$

with $\dot{Q}_R$ and L_R as the row thermal and mechanical energy flow contributions supplied or carried off. The thermal energy flow on the row hot side is simply obtained by the heat transfer balance

$$\dot{Q}_R = \bar{\alpha} S_G (\bar{T}^* - \bar{T}_W) \tag{30}$$

where $\bar{\alpha}$ is the average heat transfer coefficient, S_G is the surface area exposed to the gas with $\bar{T}^* = (T^*_i + T^*_{i+1})/2$ as the average gas temperature, and $\bar{T}_W$ as the average temperature of the material. The heat transfer coefficient is obtained as a correlation of the Nusselt number, the Reynolds number, the blade geometry, and the cooling method (film cooling, blade surface cooling mass flow ejection). The mechanical energy output L_R can be determined from the specific polytropic stage output as comprehensively discussed by Schobeiri,[14] and Schobeiri and Abouelkheir.[15]

D. Modeling of Dynamic Behavior of Shafts

The rotational speed of the ith shaft is determined by

$$\frac{d\omega_i}{dt} = \frac{1}{I_i \omega_i} (P_T - P_c - P_F - P_G)_i \tag{31}$$

where P_T, P_c, P_F, and P_G are the power of the turbine, the compressor, bearing friction, and the generator pertaining to shaft i.

E. Modeling of Plenum

Two successive components are coupled by the coupling module plenum, whose volume is made up of partial volumes of each of the two components. The temperature and pressure transients are obtained from Eqs. (4) and (5), neglecting, however, the contribution of the kinetic energy and time change in mass flow relative to other terms. This yields the following simplified relationships:

$$\frac{\partial H}{\partial t} = -\frac{\kappa}{\rho} \nabla \cdot (\rho V H) + \frac{H}{\rho} \nabla \cdot (\rho V) \tag{32}$$

$$\frac{\partial P}{\partial t} = -(k - 1) \nabla \cdot (\rho V H) \tag{33}$$

Coupling of m outlet (index O) and n inlet (index I) components and assuming one-dimensional flow results in the following two equations:

$$\frac{\partial T^*}{\partial t} = \frac{1}{\rho V} \left[\sum_{i=1}^{n} \dot{m}_{I_i} \left(\frac{c_{pI_i}}{c_p} T^*_{I_i} - T^* \right) \right] - \frac{1}{\rho V} \left[(\kappa - 1) \sum_{j=1}^{m} \dot{m}_{O_j} T^* \right] \tag{34}$$

$$\frac{\partial P}{\partial t} = \frac{\kappa R}{V} \left(\sum_{i=1}^{n} \dot{m}_{I_i} \frac{c_{pI_i}}{c_p} T^*_{I_i} - \sum_{j=1}^{m} \dot{m}_{O_j} T^* \right) \tag{35}$$

Where the nonindexed variables describe the plenum.

VI. Numerical Treatment

The above partial differential equations can be reduced to a system of ordinary differential equations by a one-dimensional approximation. The simulation of a complete gas turbine system is accomplished by combining individual components that have been modeled mathematically. The result is a system of ordinary differential equations that can be dealt with numerically. For weak transients, Runge-Kutta or predictor-corrector procedures may be used for the solution. When strong transient processes are simulated, the time constants of the differential equation system can differ so significantly that difficulties must be expected with stability and convergence of the integration methods. To avoid this problem an implicit integration method is used that is extensively discussed by Liniger and Willoughby.[16] This integration method is particularly reliable for the solution of stiff differential equations. The computer time required depends, first, on the number of components in the system and, second, on the nature of the transient processes. If the transients are very strong,

the computer time can be 10 times greater than the real time because of the halving of the time interval. For weak transients, this ratio is less than 1.

VII. Conclusions

The development of a new computational method and the corresponding generic, modularly structured computer code for simulating the nonlinear, dynamic behavior of single- and multispool high-pressure core engines, turbofan engines, and power-generation gas turbine engines is discussed in part 1 of this article. The code is capable of simulating aircraft engines having up to five spools with variable geometry, with or without additional power generation shafts. A precise prediction of the dynamic behavior of the engine and the identification of critical parameters by the presented computational method enables the engine designer to take appropriate steps using sophisticated control systems. The code may also be used to proof the design concept of the new generation of high-performance engines. In part II of this article, several critical performance assessment and validation tests were performed to ensure the capability, accuracy, robustness, and reliability of the computational method.

Acknowledgments

The authors would like to express their sincere thanks and appreciation to Carl Lorenzo, Chief System Dynamics Branch, Dan Paxson, and the administration of the NASA Lewis Research Center for the continuous cooperation and support of this project.

References

[1]Koenig, R. W., and Fishbach, L. H., "GENENG—A Program for Calculating Design and Off-Design Performance for Turbojet and Turbofan Engines," NASA TN D-6552, 1972.

[2]Seldner, K., Mihailowe, J. R., and Blaha, R. J., "Generalized Simulation Technique for Turbojet Engine System Analysis," NASA TN D-6610, Feb. 1972.

[3]Seller, J., and Daniele, C. J., "DYGEN—A Program for Calculating Steady-State and Transient Performance of Turbojet and Turbofan Engines," NASA TND-7901, April 1975.

[4]Fawke, A. J., Saravanamuttoo, H. I. H., and Holmes, M., "Experimental Verification of a Digital Computer Simulation Method for Predicting Gas Turbine Dynamic Behavior," *The Institution of Mechanical Engineers—Combustion Engines Group*, Vol. 186, No. 27, 1972, pp. 323–329.

[5]Szuch, J. R., "HYDES—A Generalized Hybrid Computer Program for Studying Turbojet or Turbofan Engine Dynamics," NASA TM X-3014, April 1974.

[6]Agrawal, R. K., and Yunis, M., "A Generalized Mathematical Model to Estimate Gas Turbine Starting Characteristics," *Journal of Engineering Power*, Vol. 104, 1982, pp. 194–201.

[7]Schobeiri, T., "Aero-Thermodynamics of Unsteady Flows in Gas Turbine Systems," Brown Boveri Co., Gas Turbine Div., BBC-TCG-51, Baden, Switzerland, 1985.

[8]Schobeiri, T., "COTRAN, the Computer Code for Simulation of Unsteady Behavior of Gas Turbines," Brown Boveri Co., Gas Turbine Div., BBC-TCG-53, Baden, Switzerland, 1985.

[9]Schobeiri, T., "Digital Computer Simulation of the Dynamic Response of Gas Turbines," *VDI—Annual Journal of Turbomachinery*, 1985, pp. 381–400.

[10]Schobeiri, T., "A General Computational Method for Simulation and Prediction of Transient Behavior of Gas Turbines," American Society of Mechanical Engineers, ASME-86-GT-180, June 1980.

[11]Schobeiri, T., "Digital Computer Simulation of the Dynamic Operating Behavior of Gas Turbines," *Journal Brown Boveri Review 3-87*, 1987, pp. 161–173.

[12]Schobeiri, H., and Haselbacher, H., "Transient Analysis of Gas Turbine Power Plants Using the Huntorf Compressed Air Storage Plant as an Example," American Society of Mechanical Engineers, ASME-85-GT-197, March 1985.

[13]Schobeiri, T., "Ein einfaches Näherungsverfahren zur Berechnung des Betriebs-verhaltens von Turbinen," *VDI-Forsch. Ing.-Wes.*, Bd. 53, Nr. 1, 1987, pp. 33–36.

[14]Schobeiri, T., "One-Dimensional Method for Accurate Prediction of Off-Design Performance Behavior of Axial Turbines," American Society of Mechanical Engineers, ASME-92-GT-54, 1992.

[15]Schobeiri, T., and Abouelkheir, M., "Row-by-Row Off-Design Performance Calculation Method for Turbines," *Journal of Propulsion and Power*, Vol. 8, No. 4, 1992, pp. 823–828.

[16]Liniger, W., and Willoughby, R., "Efficient Integration Methods for Stiff Systems of Ordinary Differential Equations," *Numerical Analysis*, Vol. 7, No. 1, 1970, pp. 47–67.